Warming, permafrost thawing and nitrogen availability are drivers of increasing plant growth and species richness on the Tibetan Plateau

Hanbo Yun[1,2,3*], Qing Zhu[4], Jing Tang[2,5,6], Wenxin Zhang[2], Deliang Chen[7], Philipp Ciais[8], Qingbai Wu[1*], Bo Elberling[2*]

[1]State Key Laboratory of Frozen Soil Engineering, Beilu'He Observation and Research Station on Tibetan Plateau, Northwest Institute of Eco–Environment and Resources, Chinese Academy of Sciences, 730000 Lanzhou, Gansu, China

[2]Center for Permafrost (CENPERM), University of Copenhagen, DK1350 Copenhagen, Denmark

[3]Department of Earth, Atmospheric, and Planetary Sciences, Purdue University, 47906 West Lafayette, Indiana, USA

[4]Climate Sciences Department, Climate and Ecosystem Sciences Division, Lawrence Berkeley National Laboratory, 94720 Berkeley, California, USA

[5]Department of Physical Geography and Ecosystem Science, Lund University, SE–22236 Lund, Sweden

[6]Department of Biology, Terrestrial Ecology, University of Copenhagen, DK–2100 Copenhagen, Denmark

[7]Department of Earth Sciences, University of Gothenburg, 41320 Gothenburg, Sweden

[8]IPSL – LSCE, CEA CNRS UVSQ UPSaclay, Centre d'Etudes Orme des Merisiers, 91191 Gif sur Yvette France

*Authors for correspondence: Hanbo Yun, hbyun@lzb.ac.cn;

Qingbai Wu, wu@lzb.ac.cn;

Bo Elberling, be@ign.ku.dk

Abstract

Permafrost-affected ecosystems are prone to warming and thawing, which can increase the availability of subsurface nitrogen (N) with consequences for otherwise N-limited tundra vegetation. Here, we show that the upper permafrost of the Tibetan Plateau is subject to thawing and that the upper permafrost zone is rich in ammonium. Furthermore, a five-year ^{15}N tracer experiment showed that long-rooted plant species were able to utilize ^{15}N-labeled N at the permafrost table and far below the main root zone. A 20 years survey is used here to document that long-rooted plant species had a competitive advantage at sites subject to warming and that both plant composition and growth were significantly correlated with permafrost thawing and changes in nitrogen availability. Our experiment documents a clear feedback mechanism of climate warming, which release plant–available N favoring long-rooted plants and explains important changes in plant composition and growth across sites on the Tibetan Plateau.

Keywords

Nitrogen, Permafrost thaw, Climate warming, Tibetan Plateau

1. Introduction

Approximately 25% of the land surface in the Northern Hemisphere is underlain by permafrost (1) and has recently warmed more than twice compared to the rest of the planet (2). This is expected to change both carbon sinks and sources and thereby the resulting net carbon–climate feedback in the tundra ecosystem (3). Tundra plant community composition and plant growth are important components of the carbon budget and have already been shown to change significantly with climate change (4, 5).

The future balance of tundra ecosystem carbon cycles has long been described as being linked to nitrogen (N) cycles, for instance, through thawing permafrost, which can release the N previously held in frozen soil layers (6–8) and thereby change the N availability for plants (9–11) and induce changes in plant growth and plant community composition (12).

Temperature (5, 13), soil moisture (12–15) and nutrition (5, 13, 16, 17) are regarded as central forces causing changes in vegetation composition and plant growth in permafrost-affected ecosystems. However, these factors reveal high spatiotemporal heterogeneity (6, 8, 12), which complicates the understanding and quantification of the mechanisms and drivers of observed changes (5, 17). This is particularly true when scaling observations across permafrost biomes and longer time scales (4, 18).

The Tibetan Plateau accounts for 75% of the Northern Hemisphere's alpine permafrost area and has experienced significant climate and environmental changes in recent decades (19, 20) as well as progressive nitrogen limitation across the Tibetan permafrost region (9). Here, we hypothesized that N released from warmer soils and permafrost thawing is available for long-rooted plant species and that subsequently plant uptake has resulted in changes in plant community composition and growth.

We performed two investigations to quantify the links between permafrost conditions and plant species composition and growth. We first quantified the plant uptake of labeled nitrogen (^{15}N) introduced at the permafrost table for 5 years. Secondly, we repeatedly quantified ambient plant species composition and plant growth based on maximum root depth, plant coverage, plant height and aboveground biomass in September and climate data linked to

active layer warming, permafrost thawing and changes in plant availability nutrients. Data were collected from 14 sites across the Tibetan Plateau (Fig. 1) between 1975 and 2017 and included 1838 soil cores from 692 plots and the corresponding plant traits.

2. Methods

Data compilation, quality control and uncertainty analysis. Air temperature, air humidity, soil temperature, soil moisture and total precipitation were obtained from the China Meteorological Data Service Center (http://data.cma.cn/) and the State Key Laboratory of Frozen Soil Engineering, China (SKLFSE; http://sklfse.nieer.ac.cn/; for details, see SI.1.1). The maximum active layer thickness (ALT) was proxied by the maximum thickness of 0 °C for yearly soil temperature. Growing degree days (GDD) were calculated by ref. 27. Soil property data and plant trait data were supported by the SKLFSE, China, and the National Cryosphere Desert Data Center, China (http://www.ncdc.ac.cn/portal/; for details, see Supplementary information (SI.)1.2). Plant species lists (presence/absence data) were made at all sites and plots from 1975, 1978, and 1995–2017 and included 87 species in total. The aboveground biomass in September was quantified from a depth of 1 cm by scissors in three 33 × 33 cm subplots within each 100 × 100 cm plot. The vertical root distribution was based on visually observed fresh roots from the flow water immersion soil core and consisted of three replicates per plot, and the mean value was calculated for the maximum root per plot (SI.1.3). Additional deep soil profile samples were collected in areas with retrogressive thaw slumps near study sites. At these sites, roots were followed to the surface and associated with species-specific living plants and maximum root lengths were recorded (SI.1.3).

The stable isotope ^{15}N data collected from 6 of the above 14 sites belonged to two groups during 2017–2021. At each site, isotopically labeled N (1 g ^{15}N–NH_4Cl, 99 atom%) was dissolved in 50 g deionized water and launched at the permafrost thaw front by a sloping drill hole (Fig. S12). The ^{15}N addition was made in five replicate plots per plant species. Roots at 0–50 cm from three dominant plant species as well as aboveground mass (including leaves and stems) were collected within 33 × 33 cm quarters immediately above the injection point. Collection also

included five additional control plots per site, and collection was made approximately ten days, one year, two years, three years and four years after the addition (SI.1.4).

After the above data collections, we conducted data quality control according to ref. 28 (SI.1.5) and uncertainty analysis to 1) examine the spatial autocorrelation in trends in variables related to weather parameters, soil properties and plant traits; and 2) assess whether different location observation years influenced the overall trends (SI.1.6 for details on how we achieved this).

Multiple regression and trend analyses. Stepwise multiple regression analysis was conducted to identify the driver of plant traits (SI.1.13). All variables were standardized by *z*–scores to facilitate comparison of model coefficients across variables with different units. Multicollinearity was checked and was well below ten for all variables (29). The R package leaps was used to select subset models, including all predictors and two–way interactions, and the skill of the model was estimated by the Akaike information criterion (AIC). The results were described by the coefficient (r^2) and *p* value, significance level <0.05.
We calculated the annual mean values of individual site and group levels for weather parameters, soil properties, soil nutrition and plant traits. The temporal trend of the weather parameter was calculated using the Mann–Kendall test with the R trend package and fitted by the ordinary least–squares method (30). The temporal trends of soil properties, soil nutrients, and plant traits were calculated using linear regression and fitted by the ordinary least–squares method (31). All significance levels were analyzed at $p < 0.05$, and the confidence level was 95%. Datasets were excluded if they were less than 10 years old.

Structure equation model (SEM). Piecewise SEM was examined to identify 1) the pathway of climate change potentially affecting plant growth and 2) the difference between the direct and indirect effects of temperature, water balance and soil nutrition on plant growth. The mean value at the site level for the growing season was used in the SEM analysis and split into two groups, A and B (Fig. S5). Variables that demonstrated a significant correlation ($p<0.05$) with plant traits in multiple regression analysis were pooled into SEM. Nutrition variation was

surrogated by the nitrogen variation, whereas ammonium (NH_4^+) variation delineated the nitrogen released from permafrost (see Supplementary SI.1.14 for justification for this assumption). Ultimately, 7 variables were used in the SEM.

All variables were standardized using *z*–scores (mean zero, unit variance). Then, principal component analysis (PCA) was used to summarize the structure between plant growth and driver parameters. We assumed linear Gaussian relationships between variables included in the model, and we tested for normality with density plots for each variable (32).

As the plant uptake nitrogen released from permafrost has a two-year time lag, the final climate change and plant trait dataset consisted of 1997 to 2017, and the soil nitrogen dataset consisted of 1995 to 2015. We fit separate models window–by–window from 0 to 5 years for growing season and non–growing season to 1) test whether the time lag of 2 years in the SEM was an artifact setting; 2) account for possible time lag effects of climate change variables (i.e., non–growing season air temperature and soil temperature) and nitrogen released from the permafrost thaw front during plant aboveground senescence.

Skill diagnostics. The goodness–of–fit of the SEMs was estimated by the chi–square (x^2), degrees of freedom (*d.f.*), and root–mean–square error of approximation (RMSEA). A path coefficient was used to sign and strengthen the relationships between two variables, which was analogous to the partial correlation coefficient or regression weight (R^2; ref. 33). The standardized total effect was calculated to quantify the contribution of all drivers to plant growth (r^2). The net influence that one variable had upon another was calculated by summing all direct and indirect pathways (effects) between two variables. All SEM analyses were conducted using the piecewiseSEM package of R.

Data Availability. All sites pf soil properties, plant traits data and R code used for the analysis used in this manuscript are publicly available from Electronic Research Data Archive (University of Copenhagen, https://www.erda.dk/), https://sid.erda.dk/sharelink/AMrPDMxk2K.

Acknowledgements. BE and HY were further supported by the Danish National Research Foundation (CENPERM DNRF 100). We thank you Dr. Anping Chen and Prof. Yiqi Luo for

suggestion about experiment design and had a level-headed review. We thank you Prof. Yongzhi Liu, Prof. Huijun Jin, Dr. Chao Mao, Guojun Liu, and Guilong Wu for field soil sample processing and laboratory analyses. We also thank Dr. Licheng Liu, and Dr. Youmi Oh for providing assistance with the structure equation model and appreciate Sebastian Zastruzny, Laura Helene Rasmussen, Emily P. Pedersen, Anne Christine Krull Pedersen, and Lena Hermesdorf for providing comments on the data analysis.

More details please see supplementary method.

3. Results

3.1 Climate change on the Tibetan Plateau

Climate data showed that the mean annual air temperature (MAAT) ranged from –4.2 to 0.8 °C from the northern to southern sites across the Tibetan Plateau and significantly increased from the study period 1975 to 2017 ($p < 0.05$; Fig. S1). The annual precipitation ranged from 83 to 460 mm in the study area, and changes over time were noted site specific at few sites (Fig. S2) and mainly during the non-growing season (Figs. S2 a and b).

The mean soil temperature of 0–100 cm was –2.5 ± 1.7 °C, and the mean soil water content (SWC) of 0–100 cm was 12.0 ± 5.3% (Fig. S3). Between 1995 and 2017, the average soil temperatures at 0–100 cm showed different responses at different sites (Fig. S3). The SWC of the 0–100 cm layer did not show significant changes at most sites, except at sites AD and KXL, which showed a significant increase during the study period.

The mean active layer thickness (ALT) of 14 sites measured at the end of the growing season from 1975 to 2017 was 248 ± 38 cm and increased by an average of 20.2 ± 4.6 cm per decade (Fig. S4). A maximum increase in ALT was observed at site QSH (35.8 cm per decade; Fig. S5), which was a relatively dry, well-drained site with low ice content at the top of the permafrost (data not shown). Sites with significant soil warming (0-100 cm) were consistent with the sites with a significant increase in ALT and vice versa for sites without significant soil warming. Based on the observed ALT trends from 1975 to 2017, the 14 study sites were split into group A with significant positive increasing trends, consisting of TSH, QSH, SQH, GZ, MA, WQ, ZAD, XD, ZD,

and HSX, and group B without significant changes, consisting of AD and BLH, and with significant negative trends, consisting of KXL and QML (Fig. S5). These two groups were hereafter used for further analyses.

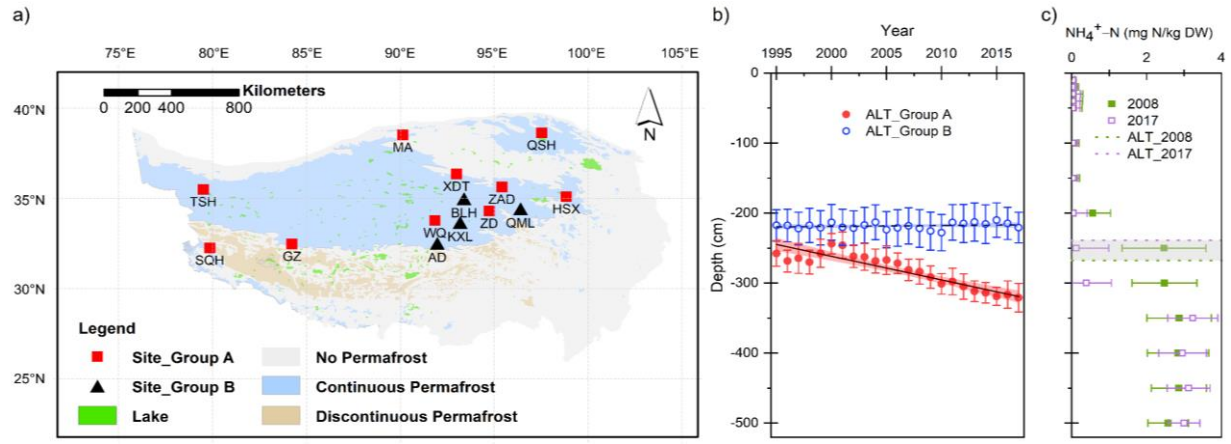

Figure 1. **a**. Map of sampling sites on the Tibetan Plateau (TSH: TianshuiHai; QSH: QingshuiHe; SQH: ShiqianHe; GZ: GaiZi; MA: MangAi; AD: AnDuo; WQ: Wen Quan; KXL: KaixinLing; BLH: BeiluHe basin; ZAD: ZaDuo; XD: XidaTan; ZD: ZhiDuo; QML: QumaLai; HSX: HuashiXia; permafrost distribution by ref. 21, 22). The boundary of the Tibetan Plateau area and permafrost distribution are based on ref. 22. Panel **b** shows the variations in active layer thickness (ALT) from 1995 to 2017 for group A (red solid dot) and group B (blue open circle). A black solid line is a significant change ($p < 0.05$), whereas a black dashed line is not significant ($p > 0.05$). Vertical bars represent one standard deviation, n = 265 for group A and n = 88 for group B. Blue and red ribbons denote the 95% confidence intervals. Panel **c** shows the NH_4^+ profiles of all 14 sites sampled at the end of September 2008 and 2017 (horizontal bars represent one standard deviation, n = 640). Light green and purple dashed lines are the mean thickness of the active layer (ALT) across sites for 2008 and 2017, respectively. The gray region denotes the variation in the permafrost thaw front from 2008 to 2017.

During the study period, on average, 83% of roots were found within the top 50 cm, 16% were within 50–100 cm, and only 1% were below 100 cm. Consequently, the active layer is discussed in the following for each of these three depth intervals (0–50 cm, 50–100 cm, and 100 cm–permafrost table). From 1995 to 2017, the soil bulk density was approximately 1.81 g cm^{-3} for the 0–50 cm, 50–100 cm, and 100 cm–permafrost tables in both group A and group B. The 0–50 cm and 50–100 cm layers showed a significant temporal trend in group A but no significant

change in group B. The 100 cm–permafrost table had no temporal trend for both groups A and B (Fig. S6 a and b). A *t*–test showed that the three layers showed no significant difference between groups A and B. Taking the depth–specific soil bulk density and the soil organic carbon (SOC) concentration into account, the SOC stock of 0–50 cm showed a significant decrease ($p < 0.01$) with a rate of 0.08 ± 0.03 kg C m^{-2} y^{-1} during 1995–2017 in group A (Fig. S7 a). This equals a total C loss of 1.8 kg C m^{-2} over 22 years or that 31% of the SOC within the top 50 cm has been mineralized within the last 20 years. With an average carbon–to–nitrogen ratio (C/N) of 10 (see below), the mineralization is expected to have released on the order of 0.2 kg N m^{-2} over the same period. However, a significant C (or N) loss has not occurred at deeper depth intervals (for group A sites; see Fig. S7 a). For the group B sites, the SOC stock (0–50 cm, 0–100 cm and 0 cm–permafrost table) showed no significant change (Fig. S7 b). Mineralization at 0–50 cm within group A sites did not result in any significant changes in soil pH (Fig. S6 g) or in any other depth intervals with group A or B sites (Fig. S6 h).

The total nitrogen (TN) stock for the group A sites in the upper 0–50 cm layer significantly decreased ($p < 0.01$), that in the 0–100 cm layer decreased ($p = 0.055$), and that in the entire active layer (0 cm to permafrost table) significantly increased during 1995–2017 ($p < 0.01$; Fig. S7 c). For the group B sites, the TN stock of the 0–50 cm, 0–100 cm, and entire active layer did not change significantly (Supplementary Fig. S7 d). The mean carbon–to–nitrogen ratio (C/N) of 0–100 cm was 10.71 ± 2.35 for group A, which significantly increased during 1995–2017 (ranging from 8.82 ± 1.01 to 13.93 ± 1.78; Fig. S7 e), and for group B, the C/N of 0–100 cm was 10.42 ± 1.75 (ranging from 9.52 ± 1.55 to 11.61 ± 2.66), showing no significant change during the same period (Fig. S7 f).

3.2 Release of nitrogen from thawing permafrost and uptake by plants

High-density drilling survey data showed that the ammonium (NH_4^+) extracted from permafrost samples (up to 500 cm below the surface) was approximately 100 times higher than that in samples in the active layer (AL) for both groups A and B from 2008 to 2017 (Fig. 1 c). This result suggests that permafrost thawing can be an important source of NH_4^+ for plant growth if

accessible via plant roots (6, 8). This assumption was further explored by an additional ^{15}N experiment.

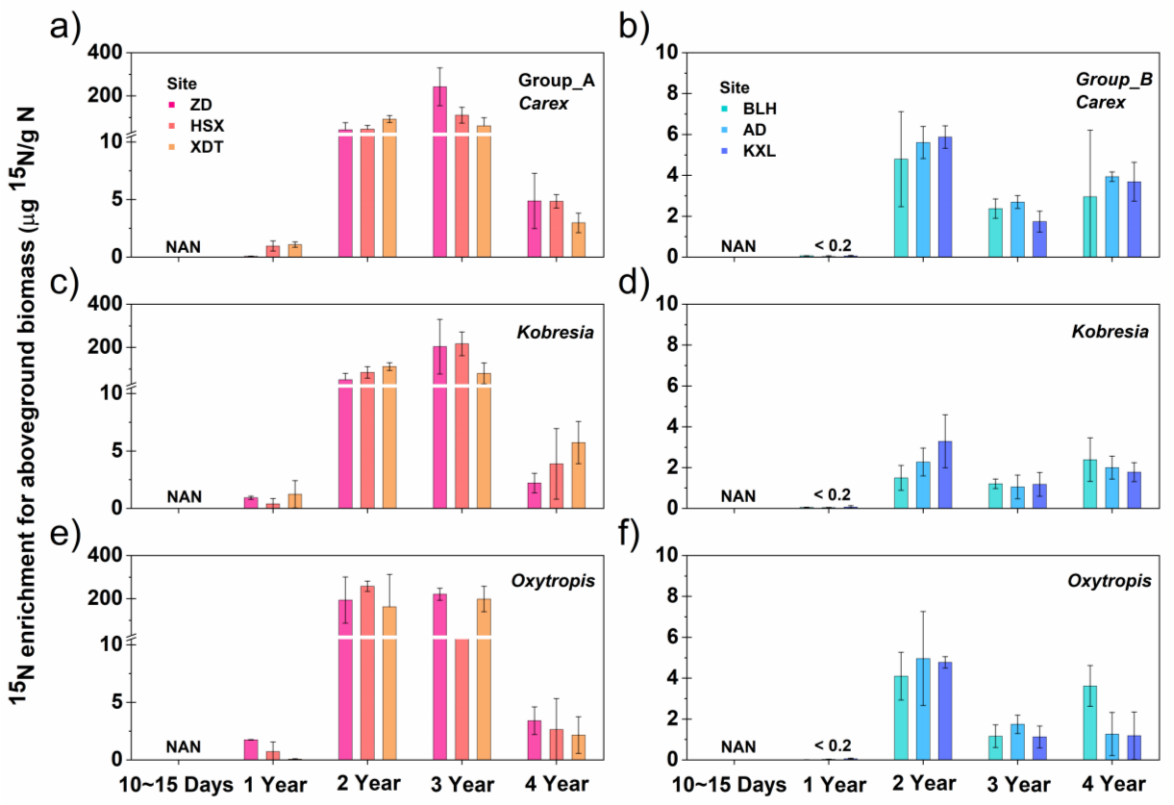

Figure 2. Enrichment $^{15}N\_NH_4$ in aboveground biomass (including leaves and stem) of long-root species (average root length between 35 to 55 cm) by treatment after 10~15 days, 1 year, 2 years, 3 years, and 4 years for group A (**a**, **c**, **e**) and group B (**b**, **d**, **f**). **a** and **b** are *Carex moorcroftii* Falc. Ex Boott (*Carex*), **c** and **d** are *Kobresia littledalei* C. B. Clarke (*Kobresia*), and **e** and **f** are *Oxytropis pauciflora* Bunge (*Oxytropis*). Vertical bars represent one standard deviation, n = 15 (after 1 year, n= 12).

To explore whether NH_4^+ released at the permafrost table in autumn is accessible to plants, a stable isotopic labeling ($^{15}N–NH_4^+$) experiment was conducted during 2017–2021. The investigation included both long-root species (root length ≥ 20 cm; Fig. 2) and shallow-root species (root length < 20 cm; Fig. S8). Our results showed that at one year after addition, plant aboveground tissue had a significant amount of labeled N (Fig. 2). This result suggests that roots can utilize N at an average depth of 3.3 m below the surface (mean thickness of the maximum active layer) and even as deep as 3.6 m below the surface at site XD, which corresponding to

the maximum active layer thickness and deepest injection depth. This is far deeper than previously reported for the Arctic (23–26) and is critical for plants living on the Tibetan Plateau. In this study, the recorded mean root depth was 24.1 ± 16.3 cm (ranging from 2.7 ± 1.2 to 103.7 ± 17.4 cm; Table S1), which was rather shallow compared with the mean ATL (248 ± 38 cm; Fig. S4). This highlights that only a few long roots are important for utilizing deep permafrost-released N. In the addition $^{15}N–NH_4^+$ experiment, nitrogen was supplied only as ammonium; however, because ammonium can be converted to nitrate through nitrification, it was not possible to conclude if plants incorporated permafrost N as ammonium or nitrate in here. The observations highlight the potential of long-rooted species benefitting from permafrost-released N compared more than shallow-rooted species.

3.3 The link between nitrogen dynamics and plant growth

Long-term trends in biologically available N and plant traits were used to assess the links between climate change-driven N dynamics and plant growth. There were 85 graminoids and 2 dwarf deciduous shrubs (*Potentilla parvifolia* Fisch. ex. Lehm. and *Myricaria prostrata* Hook. f. et Thoms. ex Benth.) recorded in group A (Table ST1), and the mean species richness increased from 15.5 species per m^2 (1995) to 23.8 species per m^2 (2010; $p < 0.1$) and then declined to 18.5 species per m^2 (2017; $p < 0.05$; Fig. S9 a). There were 62 graminoid species and one dwarf deciduous shrub (*Myricaria prostrata* Hook. f. et Thoms. ex Benth.) in group B (Table ST2), and no temporal trends were observed (with a mean species richness of 16.1 per m^2; Supplementary Fig. S9 b). From 1975–2017, the maximum root depth significantly increased from 66.8 ± 15.2 to 103.7 ± 17.4 cm in group A (Tables ST1), during which no significant change (from 62.7 ± 6.7 to 75.6 ± 5.1 cm) was noted for group B (Tables ST2). Specific species root traits were not sampled for all known plant species during the study period. However, the maximum root depths of four plant species known to have long roots were quantified in selected sites in both groups A and B (Fig. 3). For these four plant species, the maximum root depth increased significantly. For instance, *Astragalus melanostachys* roots changed from 52.1 ± 5.9 cm in 1995 to 69.7 ± 5.3 cm in 2017 at group A sites, but no significant change was observed at group B sites (Fig. 3c).

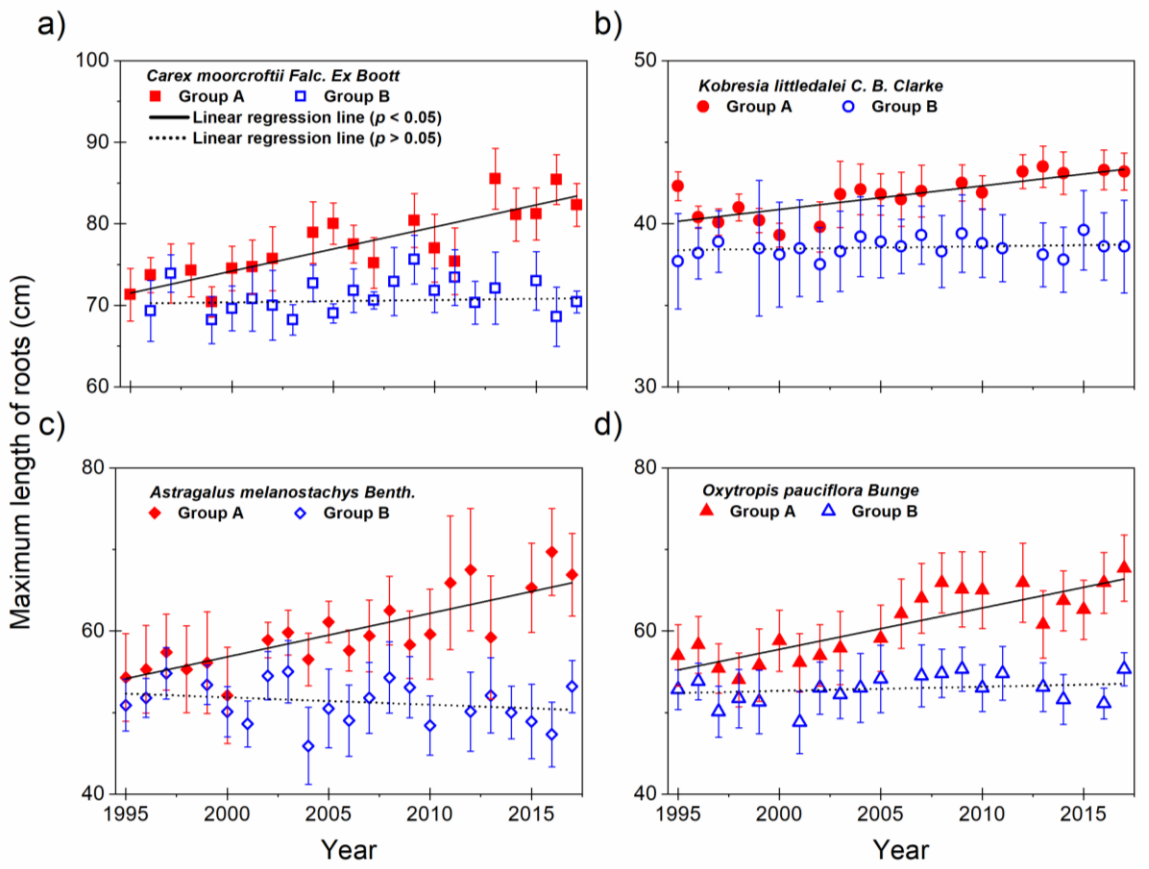

Fig. 3 Changes in maximum length of plant-specific roots for four long-rooted species for group A and group B sites from 1995 to 2017. **a** is *Carex moorcroftii* Falc. Ex Boott, **b** is *Kobresia littledalei* C. B. Clarke, **c** is *Astragalus melanostachys* Benth., and **d** is *Oxytropis pauciflora* Bunge. Vertical bars represent one standard deviation, n = 4.

At group A sites with significant permafrost thawing and active layer warming, long-rooted plant species had significantly increased root length and were able to utilize added ^{15}N at the permafrost table. Furthermore, root sampling at retrogressive thaw slumps reveled species-specific roots at least 2.4 m below the surface related to *Kobresia littledalei* C. B. Clarke and *Oxytropis pauciflora* Bunge (see SI.1.3).

The above observations show that long-rooted species have been able to utilize additional N from soils below the main root zone and suggest that N-derived from permafrost thawing can influence plant composition and plant growth. In particular, long-rooted plant species seem to have an advantage when nutrients and water are limited. This result is aligned with that in group A sites, which showed a clear relationship between the vertical maximum root depth increase ($p < 0.01$) and the species composition change, while this was, as expected, not

observed for group B sites (Fig. S9). Furthermore, convergent crossing mapping (CCM) was conducted between variations in the maximum root length and variations in the nitrogen of 50–100 cm, which had a positive correlation during 1995–2017. The CCM results showed that the direct impacts of variations in nitrogen of 50–100 cm drove the variations in maximum root length and not that root growth affected nitrogen at 50–100 cm (Fig. S10).

Subsequently, we compared the aboveground biomass in September between group A and group B from 1995 to 2017 (Table ST3). The mean aboveground biomass in September was 234.5 ± 8.0 g per m^2 for group A and 249.4 ± 6.9 g per m^2 for group B. Although the *t*–test revealed no significant differences between group A and group B, the aboveground biomass at group A sites increased significantly during 1995–2002 ($p < 0.05$) but decreased significantly during 2003–2012 ($p < 0.01$; Table ST3). For group B, the aboveground biomass did not show any significant change in either subperiod.

Interestingly, from 2008 to 2020 at permafrost thawing sites (group A), the plant species-specific results showed no consistent pattern of root length increase or biomass accumulation, either aboveground or belowground, e.g., at site XD (Fig. S11). For the species with long roots, *Anemone imbricata* Maxim. and *Oxytropis glacialis*, root length increased significantly as aboveground biomass increased, while the shallow-root species of *Leontopodium pusillum* (Beauv.) Hand.–Mazz. and *Heteropappus bowerii* (Hemsl.) Griers. showed no changes in root length or aboveground biomass. Furthermore, the root length of *Saussurea wellbyi* Hemsl. decreased significantly, while aboveground biomass increased significantly. This result suggests that shallow-root species can be affected differently by climate change than long-root species on the Tibetan Plateau. Shallow-root species may benefit from near–surface increasing mineralization linked to AL warming, while long-root species significantly increased in both root length and aboveground biomass, which could be due to the increased N availability linked to permafrost thawing.

4. Discussion

4.1 Pathway between climate change and plant community composition

To examine pathways by which climate change potentially affects plant growth and to differentiate between direct and indirect effects of temperature (air temperature, growing degree days, soil temperature of 0–50 cm, soil temperature of 50–100 cm, variation -of ALT), water balance (soil moisture of 0–50 cm, soil moisture of 50–100 cm) and soil nutrition ($N–NO_3^-$ and $N–NH_4^+$ concentration for 0–50 cm, 50–100 cm, 100 cm–permafrost front table) on plant growth, we used piecewise structural equation models (SEMs). The SEM (Fig. 4) highlighted the importance of the maximum root length (R^2=0.76) on plant growth, rather than the importance of the growing degree days (R^2=0.59) and active layer warming (R^2=0.59). The change in the maximum length of the root was roughly equally controlled by the active layer warming (R^2=0.66) and permafrost thawing (R^2=0.68).

Alleged with the additional ^{15}N experimental results, the SEM results implied that long-rooted species will benefit from AL warming and permafrost thawing, while shallow-rooted species benefit mainly from GDD. Overall, 72% of plant growth could be explained by the maximum root depth, AL warming, and GDD together, whereas 69% of the variation in the maximum root depth could be explained by AL warming and permafrost thawing alone(Fig. 4). This suggests that plant species composition in the future may depend on how different species benefit from near-surface warming versus permafrost thawing. More than 1/3 of the near–surface organic carbon has been mineralized, probably due to climate warming, which has resulted in a major near–surface inorganic N source. However, the N source linked to the permafrost table was more complex and may be available directly for plants as NH_4^+ (or NO_3^- after nitrification).

Vegetation composition changes and root dynamics in permafrost regions have important implications for ecosystem C cycling (23). The increases in root length, root exudates, and litter input may provide more C and N under warmer conditions (8, 23) as well as more N released from the permafrost table (6). The marked increase in the SOC content of the 50–100 cm layer and the change in the C/N ratio at group A sites suggest that changes in vertical root

distribution could lead to additional root litter in the 50–100 cm layer and thereby explain an increase in SOC.

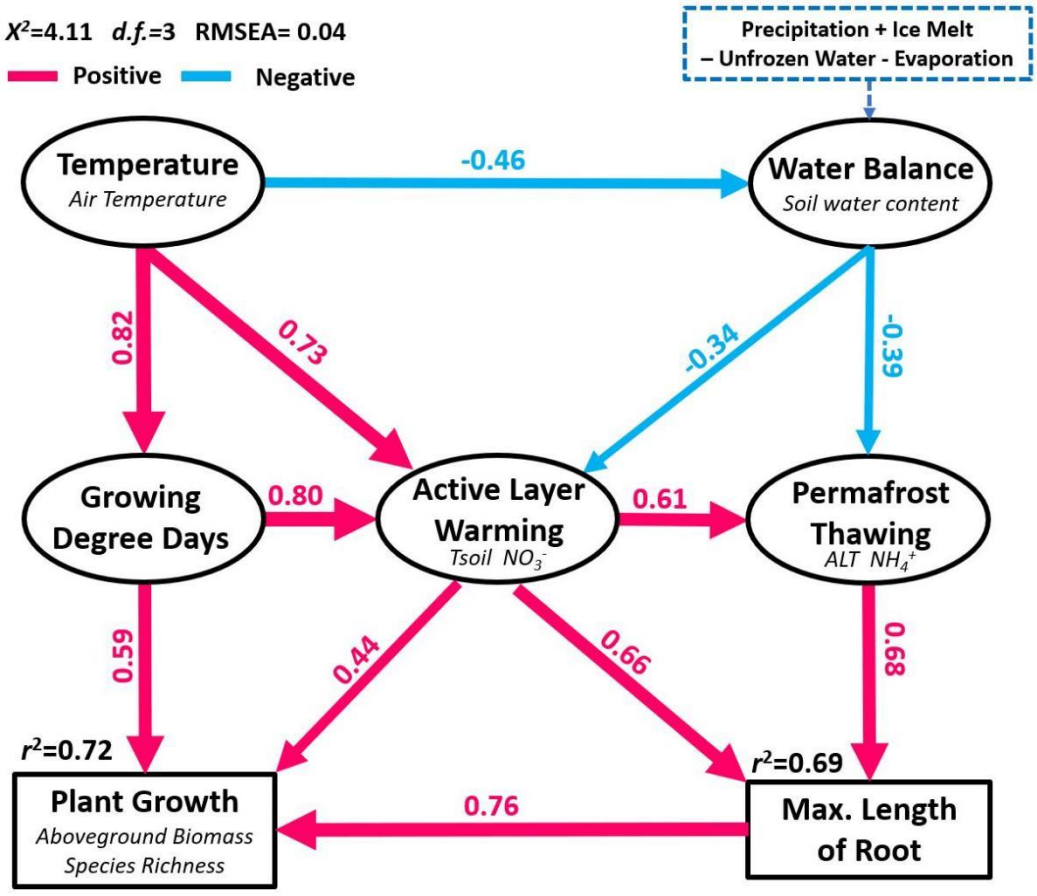

Figure 4. The structural equation model (SEM) quantifies the direct and indirect pathways of climate change on ecosystem changes measured as plant growth through additional nitrogen availability due to either active layer warming or permafrost thawing based on data from group A sites during 1995–2017. The numbers shown by the arrows are the standardized path coefficients and indicate the effect size of the relationship between two variables. Arrow widths are proportional to the path coefficient values. Only significant relationships are shown ($p < 0.05$). Red and blue arrows indicate positive and negative relationships, respectively. The chi–square statistic (χ^2), degrees of freedom (*d.f.*) and the root–mean–square error of approximation (RMSEA) are shown in the left–upper corner of the figure. For more details, please see Supplementary SI.1.14.

We conclude that (1) the permafrost layer contains higher levels of ammonium than the active layer, and ammonium is released upon thawing (nitrate can be produced in these aerated soil systems by nitrification); (2) active layer warming has resulted in corresponding enhanced soil

organic matter mineralization within the top 50 cm, and permafrost thawing with corresponding released ammonium are two important sources of inorganic nitrogen, which together is attributed to significant changes in species composition and plant growth; (3) increasing nitrogen levels corresponded to an increase in root growth and changes in plant species composition; and (4) SEM analysis indicated that climate affected plant growth (including directly and indirectly), which explained 69% of the variation in maximum root depth and 72% of the variation in plant growth. Plant variation was associated with indirect processes controlled by permafrost thawing and the associated release of plant nutrients or other factors.

In summary, climate warming has led to both warming of the AL and significant thawing of the permafrost in 10 of 14 sites across the Tibetan Plateau during the past four decades. These changes have increased the subsurface nitrogen availability from the soil surface to the permafrost table. Labeled ammonium addition (^{15}N), repeated field drilling, plant survey and SEM analysis revealed the linkage between the availability of nitrogen and a significant increase in the maximum root depth and suggested that long-rooted plant species benefitted from deeper nitrogen sources and affected species composition and aboveground plant growth. While we did not observe a significant change in aboveground biomass carbon storage at the four-decade scale, the strong trend of changing plant community composition may have important implications for biophysical feedbacks to the climate. Although this cascading biophysical effect requires further research, our findings highlight the complex interactions among climate, permafrost, nutrient cycling, and vegetation dynamics that could have lasting impacts on the ecosystem and the people of the world's highest land.

Data Availability

All sites pf soil properties, plant traits data and R code used for the analysis used in this manuscript are publicly available from Electronic Research Data Archive (University of Copenhagen, https://www.erda.dk/), https://sid.erda.dk/sharelink/AMrPDMxk2K.

Author contributions.

H.B. Yun, Q.B. Wu and B. Elberling designed project and wrote the manuscript with contributions from all authors. H.B. Yun, B. Elberling, Q. Zhu, J. Tang, W.X. Zhang and D.L. Chen

performed data analysis. P. Ciais reviewed the manuscript. H.B. Yun and Q.B. Wu collected in-situ data and finished measurements in the lab.

Competing interests.

The contact author has declared that none of the authors has any competing interests.

Acknowledgements

BE and HY were further supported by the Danish National Research Foundation (CENPERM DNRF 100). We thank you Dr. Anping Chen and Prof. Yiqi Luo for suggestion about experiment design and had a level-headed review. We thank you Prof. Yongzhi Liu, Prof. Huijun Jin, Dr. Chao Mao, Guojun Liu, and Guilong Wu for field soil sample processing and laboratory analyses. We also thank Dr. Licheng Liu, and Dr. Youmi Oh for providing assistance with the structure equation model and appreciate Sebastian Zastruzny, Laura Helene Rasmussen, Emily P. Pedersen, Anne Christine Krull Pedersen, and Lena Hermesdorf for providing comments on the data analysis.

References

1. Obu, J., et al., Northern Hemisphere permafrost map based on TTOP modelling for 2000–2016 at 1 km2 scale. *Earth Sci. Rev.*, *193*, 299-316 (2019). https://doi.org/10.1016/j.earscirev.2019.04.023
2. Parmesan, C., et al., Terrestrial and Freshwater Ecosystems and their Services. In: *Climate Change 2022: Impacts, Adaptation, and Vulnerability.* Contribution of Working Group II to the Sixth Assessment Report of the Intergovernmental Panel on Climate Change [H.-O. Pörtner, et al., (eds.)]. Cambridge University Press. In Press (2022). https://doi.org/10.5194/bg-11-6573-2014
3. Virkkala, A. M., et al., Statistical upscaling of ecosystem CO2 fluxes across the terrestrial tundra and boreal domain: Regional patterns and uncertainties. *Glob. Chang. Biol.*, *27*(17), 4040-4059(2021). https://doi.org/10.1111/gcb.15659
4. Bjorkman, A. D., et al., Plant functional trait change across a warming tundra biome. *Nat.*, *562*(7725), 57-62(2018). https://doi.org/10.1038/s41586-018-0563-7
5. Niittynen, P., Heikkinen, R. K., & Luoto, M., Snow cover is a neglected driver of Arctic biodiversity loss. *Nat. Clim. Chang.*, *8*(11), 997-1001(2018). https://doi.org/10.1038/s41558-018-0311-x
6. Elberling, B., Christiansen, H. H., & Hansen, B. U., High nitrous oxide production from thawing permafrost. *Nat. Geosci.*, *3*(5), 332-335(2010). https://doi.org/10.1038/ngeo803
7. Keuper, F., et al., Experimentally increased nutrient availability at the permafrost thaw front selectively enhances biomass production of deep-rooting subarctic peatland species. *Glob. Chang. Biol.*, *23*(10), 4257-4266 (2017). https://doi.org/10.1111/gcb.13804
8. Salmon, V. G., et al., Adding depth to our understanding of nitrogen dynamics in permafrost soils. *J. Geophys. Res. Biogeosci.*, *123*(8), 2497-2512(2018).

https://doi.org/10.1029/2018JG004518

9. Kou, D., et al., Progressive nitrogen limitation across the Tibetan alpine permafrost region. *Nature communications*, 11(1), 1-9 (2020). https://doi.org/10.1038/s41467-020-17169-6
10. Hewitt, R. E., Taylor, D. L., Genet, H., McGuire, A. D., & Mack, M. C. Below-ground plant traits influence tundra plant acquisition of newly thawed permafrost nitrogen. *J. Ecol.*, *107*(2), 950-962(2019). https://doi.org/10.1111/1365-2745.13062
11. Pedersen, E. P., Elberling, B., & Michelsen, A. Foraging deeply: Depth-specific plant nitrogen uptake in response to climate-induced N-release and permafrost thaw in the High Arctic. *Glob. Chang. Biol.*, *26*(11), 6523-6536(2020). https://doi.org/10.1111/gcb.15306
12. Heijmans, M. M., et al., Tundra vegetation change and impacts on permafrost. *Nat. Rev. Earth Environ.*, *3*(1), 68-84(2022). https://doi.org/10.1038/s43017-021-00233-0
13. Elmendorf, S. C., et al., Plot-scale evidence of tundra vegetation change and links to recent summer warming. *Nat. clim. Chang.*, 2(6), 453-457(2012). https://doi.org/10.1038/nclimate1465
14. Kemppinen, J., Soil moisture and its importance for tundra plants (2020). http://urn.fi/URN:ISBN:978-951-51-4933-6
15. Happonen, K., Virkkala, A. M., Kemppinen, J., Niittynen, P., & Luoto, M., Relationships between above‐ground plant traits and carbon cycling in tundra plant communities. *J. Ecol.*, 110(3), 700-716(2022). https://doi.org/10.1111/1365-2745.13832
16. Schuur, E. A., Crummer, K. G., Vogel, J. G., & Mack, M. C., Plant species composition and productivity following permafrost thaw and thermokarst in Alaskan tundra. *Ecosyst.*, *10*(2), 280-292(2007). https://doi.org/10.1007/s10021-007-9024-0

17. Myers-Smith, I. H., et al., Eighteen years of ecological monitoring reveals multiple lines of evidence for tundra vegetation change. *Ecol. Monogr.*, *89*(2), e01351(2019). https://doi.org/10.1002/ecm.1351
18. Thomas, H. J., et al., Global plant trait relationships extend to the climatic extremes of the tundra biome. *Nat. Commun.*, *11*(1), 1-12(2020). https://doi.org/10.1038/s41467-020-15014-4
19. Chen, D., et al., Assessment of past, present and future environmental changes on the Tibetan Plateau. *Chin. Sci. Bull*., 60(32), 3025-3035(2015). https://doi.org/10.1360/N972014-01370
20. Yao, T., et al., Recent third pole's rapid warming accompanies cryospheric melt and water cycle intensification and interactions between monsoon and environment: Multidisciplinary approach with observations, modelling, and analysis. *Bull. Am. Meteorol. Soc.*, 100(3), 423-444(2019). https://doi.org/10.1175/BAMS-D-17-0057.1
21. Wang, T., et al., Permafrost thawing puts the frozen carbon at risk over the Tibetan Plateau. *Sci. Adv.*, 6(19), eaaz3513(2020). https://doi.org/10.1126/sciadv.aaz3513
22. Zou, D., et al., A new map of permafrost distribution on the Tibetan Plateau. *Cryosphere*, *11*(6), 2527-2542(2017). https://doi.org/10.5194/tc-11-2527-2017
23. Blume-Werry, G., Milbau, A., Teuber, L. M., Johansson, M., & Dorrepaal, E., Dwelling in the deep–strongly increased root growth and rooting depth enhance plant interactions with thawing permafrost soil. *New Phytol.*, *223*(3), 1328-1339(2019). https://doi.org/10.1111/nph.15903
24. Finger, R. A., et al., Effects of permafrost thaw on nitrogen availability and plant–soil interactions in a boreal Alaskan lowland. *J. Ecol.*, *104*(6), 1542-1554(2016). https://doi.org/10.1111/1365-2745.12639

25. Abramoff, R. Z., & Finzi, A. C., Are above-and below-ground phenology in sync?. *New Phytol.*, *205*(3), 1054-1061(2015). https://doi.org/10.1111/nph.13111
26. Riley, W. J., Zhu, Q., & Tang, J. Y., Weaker land–climate feedbacks from nutrient uptake during photosynthesis-inactive periods. *Nat. Clim. Chang.*, *8*(11), 1002-1006(2018). https://doi.org/10.1038/s41558-018-0325-4
27. Bendixen, M., et al., Delta progradation in Greenland driven by increasing glacial mass loss. *Nat.*, *550*(7674), 101-104. (2017). https://doi.org/10.1038/nature23873
28. Essington, T., et al., Historical reconstruction of the Puget Sound (USA) groundfish community. *Mar. Ecol. Prog. Ser*., 657, 173-189(2021). https://doi.org/10.3354/meps13547
29. Queen, J. P., Quinn, G. P., & Keough, M. J., *Experimental design and data analysis for biologists*. Cambridge university press (2002).
30. Essington, T. E., *Introduction to Quantitative Ecology: Mathematical and Statistical Modelling for Beginners*. Oxford University Press (2021).
31. Pinheiro, J. C., & Bates, D. M., Linear mixed-effects models: basic concepts and examples. Mixed-effects models in S and S-Plus, Statistics and Computing. Springer, 3-56(2000). https://doi.org/10.1007/0-387-22747-4_1
32. Grace, J. B., Structural equation modeling and natural systems. Cambridge University Press (2006).
33. Mallet, A. A., A maximum likelihood estimation method for random coefficient regression models. *Biometrika*, 73(3), 645-656(1986). https://doi.org/10.1093/biomet/73.3.645